Korean J. Chem. Eng., 40(7), 1731-1745 (2023)
DOI: 10.1007/s11814-023-1424-0

pISSN: 0256-1115
eISSN: 1975-7220

Towards improved removal of multicomponent from wastewater using a predefined multistage direct pass of reverse osmosis

Mudhar A. Al-Obaidi[*,**,†]

*Middle Technical University (MTU), Technical Institute of Baquba, Baquba, Dayala - Iraq
**Middle Technical University, Technical Instructor Training Institute, Baghdad - Iraq
(*Received 6 November 2022 • Revised 7 January 2023 • Accepted 31 January 2023*)

Abstract−The vast growth of the manufacturing world is producing a massive amount of wastewater from a wide range of industrial applications disposed into surface water. Undoubtedly, these effluents contain a variety of high-toxic compounds that pose a real challenge and dislocate the environment. The reverse osmosis (RO) process is recognized as a superior method due to its reliability in generating a roughly pure reuse water at a plausible cost. However, the literature has a shortage of comprehensive studies to simultaneously eliminate organic and non-organic compounds from wastewater using a predefined multi stage direct pass operation of a spiral wound module of RO process. To systematically carry out this, a mathematical model developed by the same author has been modified to critically predict the efficiency of RO process towards the simultaneous removal of multi-component from wastewater. For this system, the simulation introduces realistic operating circumstances that correspond to a high rejection of the targeted chemicals. By optimizing the design operating conditions, the accompanying treatment process' consistency and effectiveness are also increased. As a result, there was a noticeable decline in the unintended release of the harmful substances into the recycled water within a fixed specific energy consumption.

Keywords: Wastewater Treatment, Spiral Wound RO Process, Simulation, Optimization, Multicomponent Removal

INTRODUCTION

The presence of numerous harmful organic and inorganic chemicals in industrial effluent is the main problem. Therefore, it is strongly advised to recover these chemicals from industrial effluents. Pesticides, petrochemicals, and pharmaceutical companies all produce waste that contains a variety of very dangerous substances, including phenol and its derivatives [1]. Interestingly, several wastewater conventional treatment technologies are used to deactivate these pollutants from wastewater, such as such as UV oxidation, biological, electrochemical, and adsorption processes [2]. Most of these treatments come with high energy and energy consumption [3]. In line with this, the reverse osmosis (RO) process has been ascertained as an efficient technology working at a plausible treatment cost for several compounds in advanced water reclamation [4,5]. The RO process is a clean technology for the treatment of effluents coming from several industries without the addition of any chemicals. Specifically, the spiral wound (SW) module has been widely used in several industries as the prominent design for its high removal efficiency at easy operation at low fouling propensity [6].

A number of attempts can be found in the literature for mathematically modelling and simulating the spiral wound module of the RO process and examine its feasibility in the deletion of a single or multi organic or non-organic compounds from wastewater.

A successful lumped model was established by Al-Bastaki [7] and used to assess the performance of a spiral wound module of RO process via a simulation to remove methyl orange dye and sodium sulfate salt from wastewater under different feed concentration. It has been stated that increasing the feed concentration has resulted in a decrease of solute rejection.

Ahmad et al. [8] did experimental work to assess the performance of a pilot-plant RO process of PVDF membrane module ($0.9\ m^2$) for the removal of a multiple solute system of organic matters, including oil and grease, carbohydrate, and protein from palm oil mill effluent. The simulation based unsteady state model of RO process ascertained the reduction of permeate flux throughout the operational time. The RO process has successfully removed the associated constituents and achieved the desired water quality.

Due to the undesirable effect of salts, organic matters and nutrients, Al-Rifai et al. [9] studied during a one-year the performance of a full-scale of combined microfiltration and RO processes to treat real wastewater of an actual water recirculation plant containing thirteen endocrine disrupting compounds and pharmaceutically active compounds. Except bisphenol, this study assured the reliability of MF/RO system for the elimination of targeted compounds with a significant reduction in the treated water.

A full scale plant of three RO stages of spiral wound modules connected in a series was used by Fujioka et al. [10] to evaluate the remove eight compounds of N-nitrosamine family from wastewater with appraising the influence of feed temperature. This, in turn, showed variable rejections of the components attributed to the influence of feed temperature and different feed concentrations. Also, it has been concluded that there is a substantial difference in rejecting the N-nitrosamine compounds throughout the connected stages

†To whom correspondence should be addressed.
E-mail: dr.mudhar.alaubedy@mtu.edu.iq

of RO process.

Wang et al. [11] appraised the efficiency of a sequential five stages of individual low-pressure spiral wound modules of RO process to remove seven disinfection by-products of halo-acetic acids and NaCl from produced water of a water drinking system. The simulation showed that increasing the pressure has positively increased the water recovery while decreasing the rejection of halo-acetic acids.

Al-Obaidi et al. [12] presented a simple model of a single spiral wound module (7.84 m^2) of RO process to remove a number of non-organic and organic species from a synthesized wastewater. The simulation of the RO process obtained the overall rejection of each compound while the optimization enabled to predict the optimal operating conditions to find the optimum rejection of each compound.

Domingos et al. [13] tested the feasibility of a pilot scale of a combination of three spiral wound modules stuffed with TFC polyamide membranes (0.38 m^2) and two nanofiltration cartridges to treat synthetic wastewater of high-concentrations of volatile fatty acids. The influence of different operating conditions on the overall rejection was studied. The pressure and temperature were identified to have a positive influence on water flux with insignificant effect of pH. More importantly, the RO process with a batch concentration mode has enabled concentrating the feed solution three times with less than 4% concentration of volatile fatty acids in the permeate side.

A precise review of the previous literature would ascertain the need to analyze and assess the viability of a multistage direct pass operation RO process towards the simultaneous removal of a number of organic and non-organic compounds of synthesized wastewater. Thus, the purpose of this study is to utilize a moderated version of an earlier model of RO process developed by the same author to enable the prediction of simultaneous elimination of a complex wastewater of several organic and non-organic compounds using a predefined multistage direct pass operation of RO process. Due to the deficiency of detailed experimental data for the treatment of wastewater using spiral wound direct pass operation RO process, the model developed in this study has been corroborated in terms of observational data gathered from the literature for the rejection of a single pollutant (chlorophenol) from wastewater. Then, a comprehensive study was conducted to evaluate the removal of each compound under variable sets of operating conditions. This, in turn, has provided a deep understanding on the process performance and elucidated the influence of operating conditions on the rejection of each considered pollutant. Finally, the model developed is imbedded in a nonlinear multi-objective function optimization to find the optimal inlet conditions of a direct pass operation multistage RO process and simultaneously elevate the removal of the selected compounds and promote the average recovery rate.

DESCRIPTION OF MULTISTAGE RO PROCESS AND ASSOCIATED ADVANTAGES MULTICOMPONENT WASTEWATER

A schematic diagram of the proposed multistage direct pass operation of RO process is shown in Fig. 1. This is specifically containing three stages of RO process connected in a series configuration, where the disposed stream of the first stage is the feed of the second stage and so on. The tapered configuration of 3 : 2 : 1 of pressure vessels is selected in this study where each pressure vessel holds one membrane. The membrane characteristics are provided in Table 1. The direct pass operation of RO stages is characterized by decreasing the number of pressure vessels from the first stage to the last stage. This is important to suit the decrease of volume flowrate from the former stage to the latter one which continuously converted into permeate. In this regard, the permeates of all stages are combined to form the main permeate stream. A high-pressure pump of 85% efficiency (ε_{pump}) is used to drive the wastewater into the RO process.

The direct pass operation of a multistage RO process allows a continuously discharging of retentate and permeate into retentate and permeate tanks without recycling one or both these steams. It is believed that recycling the retentate and permeate streams into the feed tank as a total recirculation mode requires the utilization of a larger feed pump to handle high feed flowrate that ascertains a high specific energy consumption. Furthermore, recycling a part or the whole retentate stream into the suction of the high pressure pump of feed stream in a batch mode would increase the feed concentration with the operational time with a high propensity of membrane fouling and high concentration of permeate despite the opportunity to elevate the overall water recovery [13]. This in turn would justify the selection of the direct pass operation of RO pro-

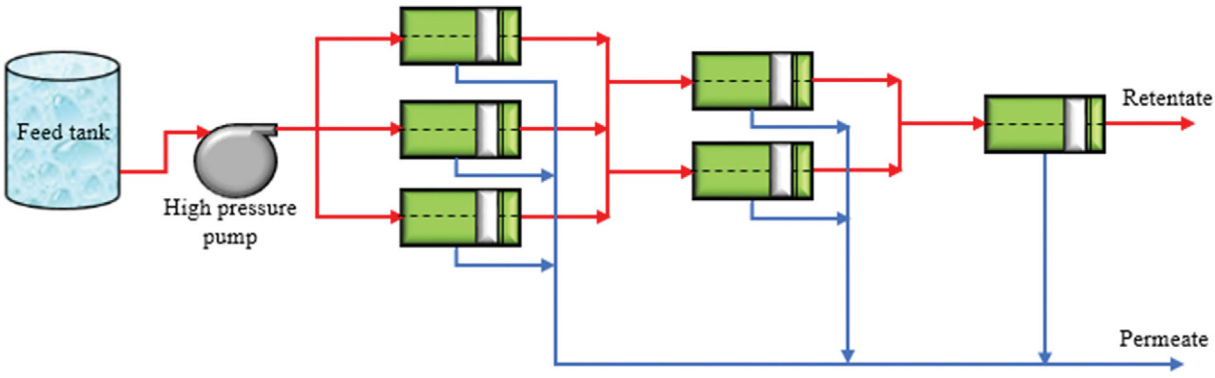

Fig. 1. A schematic diagram of a predefined (3 : 2 : 1) direct pass operation of RO process.

Table 1. The characteristics of a single spiral wound membrane module of RO process

Individual membrane properties	Value	Unit
Membrane brand and supplier	TM820M-400/SWRO, Toray membrane	-
Membrane material and module configuration	Polyamide thin-film composite spiral wound element	-
Effective membrane area (A_m), module width (W) and length (L)	37.2, 37.2, and 1	m^2, m, m
Water transport parameter ($A_{w(T_o)}$) at 25 °C *	3.159×10^{-7}	m/s atm
Maximum and minimum feed flow rate	463.104 and 86.4	m^3/day
Maximum operating temperature	45	°C
Maximum pressure	81	atm
Feed spacer thickness (t_f)	8.6×10^{-4} (34 mils)	m
Length of filament in the spacer mesh (L_f)	2.77×10^{-3}	m
Hydraulic diameter of the feed spacer channel (d_h)	8.126×10^{-4}	m
Spacer characteristics (A′) and (n^*)	7.38 and 0.34	-
Membrane porosity (ε)	0.9058	-

*: Used by Filippini et al. [14] and Al-Obaidi et al. [15]

cess in this study that would mitigate the specific energy consumption with improving the water recovery. Furthermore, the multistage RO process is considered in this study compared to an individual module of a spiral wound module of RO process due to the capacity of improving the overall water recovery.

THE PROPOSED MULTICOMPONENT WASTEWATER

The proposed wastewater of this study comprises a combination of organic, non-organic and salt matters. These are specifically three inorganic matters of cyanide, ammonium, and sulfate, and four organic matters of chlorophenol, dimethylphenol, phenol, N-nitrosodimethylamine-D6 and aniline and NaCl (salt). Note that the selected compounds are released in the industrial wastewater of a wide set of industrial applications and cause serious environmental pollution. For instance, aniline derivatives are commonly deployed in the industry of drugs, dyes, pigments, and pesticides [16]. Also, phenol (aromatic compound), is one of most prevalent pollutants found in the wastewater of disinfectants, pharmaceuticals industries [17]. Table 2 presents the solute transport parameters of the associated compounds. Note that the solute transport parameter is an indicator of the transportation affinity of the solute from the feed side to the permeate side throughout the membrane pores. Increasing the solute transport parameter simply means a higher opportunity to be moved and collected in the permeate side.

Table 2. Solute transport parameters of the selected chemicals

Compound	B_s (m/s)	References
Cyanide	2.186×10^{-6}	[18]
Aniline	4.190×10^{-6}	[19]
Ammonium	1.169×10^{-7}	[20]
Phenol	6.536×10^{-7}	[21]
Chlorophenol	8.468×10^{-8}	[22]
Dimethylphenol	2.225×10^{-8}	[21,23]
N-nitrosodimethylamine-D6	5.35×10^{-6}	[24]
Sulphate	3.987×10^{-8}	[25]
NaCl	1.749×10^{-8}	[14]

MODEL RATIONALE AND DEVELOPMENT

Table A1 of Appendix A presents the model equations of the model developed by the same author [14,15] to characterize the overall performance of a single spiral wound membrane of RO process applied for seawater desalination. The model equations corresponding to the performance evaluations of multistage RO process are also presented in Table A2 of Appendix A including the streams connections. Recently, this model was moderated to estimate the removal of multicomponent from wastewater via the multistage RO process. The model is generally based on the principles of solution diffusion model and the film theory to elucidate the permeate and solutes fluxes through the membrane and justify the concentration polarization effect. Due to the multicomponent nature of the wastewater, the influence of all the quantified compounds to the osmotic pressure was included. However, the water and solute transport parameters of the associated pollutants were assumed constant along the feed channel. The physical properties of multicomponent wastewater were estimated based on the seawater properties including the diffusivity, viscosity, and density. This is due to considering the low concentrations of pollutants in the wastewater.

The model of multistage RO process based wastewater treatment is coded and solved in MATLAB software and then used to carry out simulation and optimization studies.

MODEL VALIDATION

To confirm the robustness of the model developed in this study, the performance indicators of multistage RO process of eight pressure vessels were connected in a series configuration; each pressure vessel holds one spiral wound membrane (TM820M-400/SWRO, Toray), and using Toray Design System 2 (TDS2) are compared to the model predictions of the recent model. The associated results

Table 3. Comparison between the results of TDS2 data and the model predictions of 8 membranes in a series configuration

Inlet conditions	Performance indicators	Model predictions (this work)	TDS2 Data	Error%
($C_{f(plant)}$=35,000 ppm) ($P_{f(plant)}$=48.69 atm) ($Q_{f(plant)}$=6,145.80 m^3/day) ($T_{(plant)}$=25 °C)	$C_{p(plant)}$ (ppm)	389.8	385.8	−1.036
	$C_{r(plant)}$ (ppm)	58,127.08	58,074.47	−0.090
	$Q_{p(plant)}$ (m^3/day)	2,461.79	2,457.56	−0.172
	$Q_{r(plant)}$ (m^3/day)	3,684.18	3,688.76	0.124
	$P_{r(plant)}$ (atm)	44.05	43.71	−0.787
	$Rec_{(plant)}$ (-)	40.05	42	4.629
	$Rej_{(plant)}$ (-)	98.88	98.89	0.011
($C_{f(plant)}$=35,000 ppm) ($P_{f(plant)}$=52.91 atm) ($Q_{f(plant)}$=6,480 m^3/day) ($T_{(plant)}$=25 °C)	$C_{p(plant)}$ (ppm)	351.18	365.8	3.996
	$C_{r(plant)}$ (ppm)	63,569.08	63,333.42	−0.372
	$Q_{p(plant)}$ (m^3/day)	2,928.36	2,916.00	−0.423
	$Q_{r(plant)}$ (m^3/day)	3,551.56	3,564.00	0.349
	$P_{r(plant)}$ (atm)	47.97	47.97	−0.570
	$Rec_{(plant)}$ (-)	45	45	−0.425
	$Rej_{(plant)}$ (-)	98.95	98.9548	−0.042

Note: $C_{f(plant)}$ denotes the total dissolved salts of inlet water.

Table 4. Fixed and range of variation of operating conditions for sensitivity analysis

Parameter	Fixed value	Variation
Feed concentration of selected pollutants (ppm)	500	300-1,000
Feed concentration of N-nitrosodimethylamine-D6 (ng/l)	500	300-1,000
Feed concentration of NaCl (ppm)	1,000	500-1,500
Feed pressure (atm)	20	10-40
Feed flow rate (m^3/day)	777.6	259.2-1,296
Feed temperature (°C)	25	20-35

of two specific sets of inlet conditions, presented in Table 3, show relatively small errors for most performance indicators.

SENSITIVITY ANALYSIS OF OPERATING CONDITIONS

The most crucial parameters that directly affect the performance indicators must be found by using the sensitivity analysis of the RO system. Thus, it is important to analyze the process performance when input parameters are varied through a sensitivity analysis. This is useful both to design the membrane unit at the lowest specific energy consumption considering various locations for its installation (i.e., different wastewater quality and temperature) and to predict the results of an expected disturbance on the performance (i.e., change of inlet pressure, flow rate, concentration, and temperature).

The simulation of this paper was carried out using a model developed by Filippini et al. [14] and Al-Obaidi et al. [15] for a single spiral wound of RO process. The model was calibrated to investigate the performance indicators of the proposed design of Fig. 1. This would ensure the calculations of several performance indicators of overall rejection, product salinity, recovery, and specific energy consumption. These parameters are defined as follows.

- Percentage recovery ratio of the plant (Rec %), which is the quantity of permeate produced over the quantity of feed introduced.
- Percentage plant salt rejection (Rej %), which indicates the ability of the plant to reject the solute in the feed via the membrane.
- Specific energy consumption (SEC), which is essential to pump the feed water into the RO system and mainly directed to operating pressure and flow rate [26]. Specifically, SEC is an important indicator of the operating expenses of the process.

In this respect, the fixed input parameters of feed pressure, concentration, flow rate and temperature used in sensitivity analysis in addition to the selected range of input parameters are given in Table 4.

To examine the influence of a specific input parameter on the performance metrics of the RO system, the sensitivity analysis was achieved by varying one parameter at a time while other parameters were fixed. Note that the input parameters of feed pressure and temperature are selected within the allowed upper and lower limits recommended by the manufacturer for the used membrane type (Table 1). However, the operating feed flow rate was considered based on the number of parallel pressure vessels of the first stage (i.e., three pressure vessels) and the allowed upper and lower limits recommended by the manufacturer of feed flow rate for the specific membrane used. Furthermore, the feed concentrations of the considered compounds, N-nitrosodimethylamine-D6 and NaCl, were taken between 300-1,000 ppm, 300-1,000 ng/l and 500-1,500 ppm, respectively, to simulate actual wastewater of a wide set of industrial applications. As a by-product of disinfection with chlo-

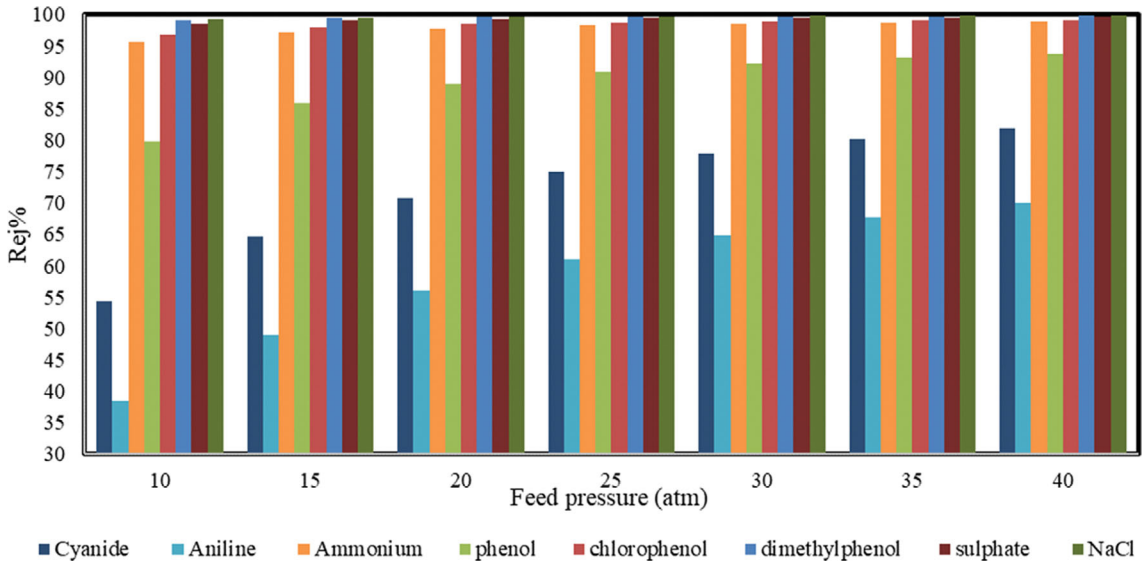

Fig. 2. Variation of solute rejection of different species against feed pressure at fixed feed flowrate, concentration of pollutants, and temperature (inlet concentration of each pollutant (500 ppm), feed flowrate (777.6 m^3/day), and temperature (25 °C)).

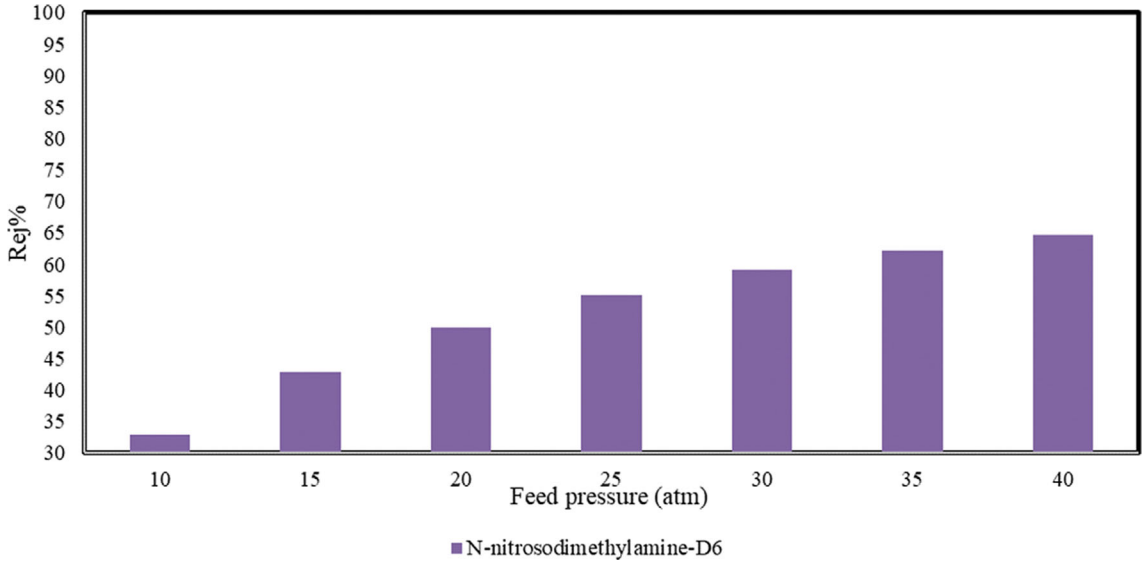

Fig. 3. Variation of N-nitrosodimethylamine-D6 rejection against feed pressure at fixed feed flowrate, concentration, and temperature (inlet concentration of N-nitrosodimethylamine-D6 (500 ng/l), feed flowrate (777.6 m^3/day), and temperature (25 °C)).

ramine of water or wastewater effluents containing dimethylamine, N-nitrosodimethylamine-D6 can exceed 790 ng/l in the samples from wastewater treatment plants and industrial sources [27]. However, the untreated wastewater and sewage water often contain significant concentrations of N-nitrosodimethylamine-D6. In this regard, Srinivasan et al. [28] used the range between 100-800 ppm of dimethylphenol to carry out an experimental study on the removal of dimethylphenol in a lab scale RO process. To mimic the wastewater of chemical, pharmaceutical and petrochemical industries, Cui et al. [29] studied the efficiency of lab-fabricated forward osmosis and RO modes for the removal of organic micro-pollutants from wastewater. The feed concentrations of phenol, aniline and nitrobenzene were varied between 500-2,000 ppm of each pollutant.

The influence of inlet pressure on solute rejection of different pollutants at a fixed set of inlet concentration of each pollutant (500 ppm) and 500 ng/l of N-nitrosodimethylamine-D6, feed flowrate (777.6 m^3/day), and temperature (25 °C) is shown in Figs. 2 and 3. Specifically, the increase of feed pressure from 10 atm to 30 atm causes an exponential rise of the rejection parameter. In this respect, N-nitrosodimethylamine-D6, aniline, cyanide, and phenol have noticed a clear increase of rejection compared to other pollutants. Statistically, the rejections of N-nitrosodimethylamine-D6, aniline, cyanide, and phenol increase by around 95%, 82%, 51%, and 17%, respectively, compared to only 4% increase in the ammonium rejection for the specified range of feed pressure. Increasing the pressure drives more water to penetrate water through the membrane pores,

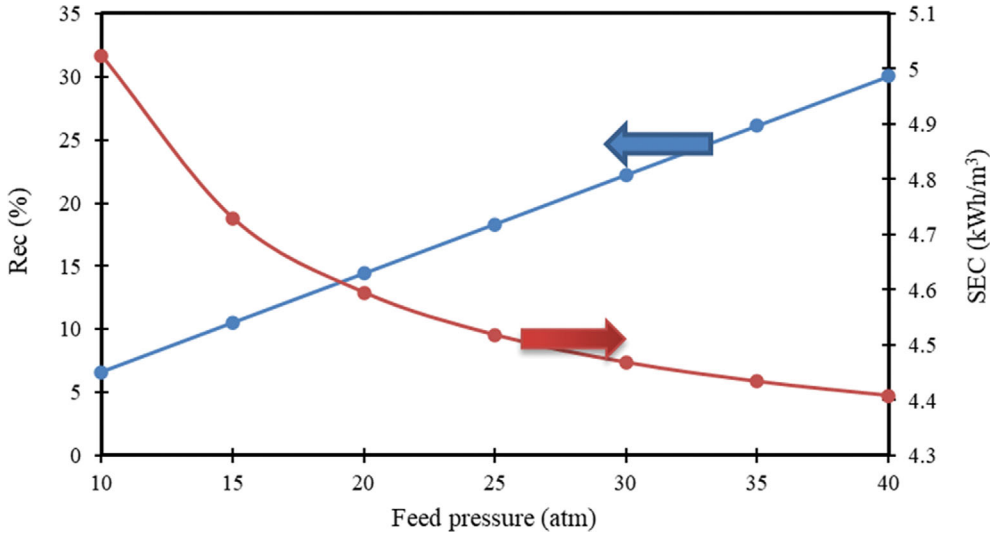

Fig. 4. Variation of water recovery and specific energy consumption against feed pressure at fixed feed flowrate, concentration, and temperature (inlet concentration of each pollutant (500 ppm), concentration of N-nitrosodimethylamine-D6 (500 ng/l), feed flowrate (777.6 m^3/day), and temperature (25 °C)).

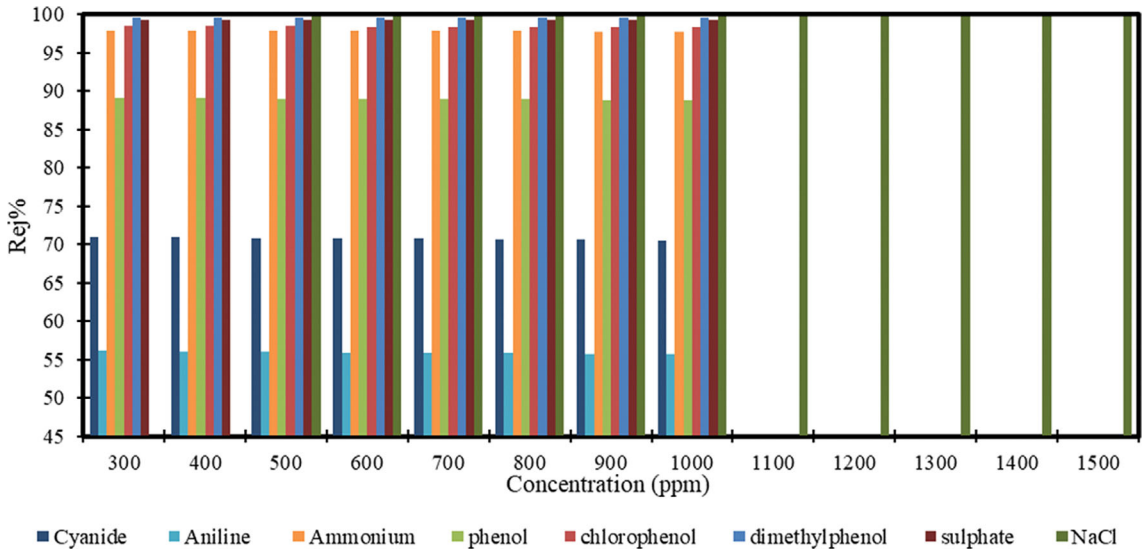

Fig. 5. Variation of solute rejection of different species against inlet feed concentration of pollutants at fixed feed flowrate, pressure, and temperature (inlet pressure (20 atm), feed flowrate (777.6 m^3/day), and temperature (25 °C)).

which dilutes the pollutant's concentration in the permeate channel and therefore enhances the rejection.

The overall water recovery and specific energy consumption for the selected configuration of RO system (Fig. 1) are schematically presented in Fig. 4. As stated above, increasing feed pressure has increased the driving force of water penetration due to enlarging the difference between feed pressure and osmotic pressure. This, in turn, causes a substantial increase in permeated flow rate that collected as treated water from the permeate channel. At fixed inlet flow rate, this would interpret the steady increase of water recovery against feed pressure besides the importance of feed pressure as a key parameter for enhancing the operation of RO process. Based on Eq. (18) of Table A2, increasing permeate flow rate at fixed inlet feed flow rate would reduce the specific energy consumption. Clearly, Fig. 4 shows an exponential decrease of specific energy consumption against feed pressure. These findings corroborate the results of Karabelas et al. [30] who evaluated the influence of different factors to energy consumption in spiral wound membranes of RO desalination process including the feed pressure.

To evaluate the influence of feed concentration of pollutants on the overall rejection of these pollutants at a fixed set of inlet pressure (20 atm), feed flowrate (777.6 m^3/day), and temperature (25 °C), Figs. 5 and 6 show the simulation result of pollutants' and N-nitrosodimethylamine-D6′ rejections, respectively. Obviously, Figs. 5 and 6 ascertain the inconsiderable impact of feed concentration on the rejection of the tested pollutants for the tested range of feed con-

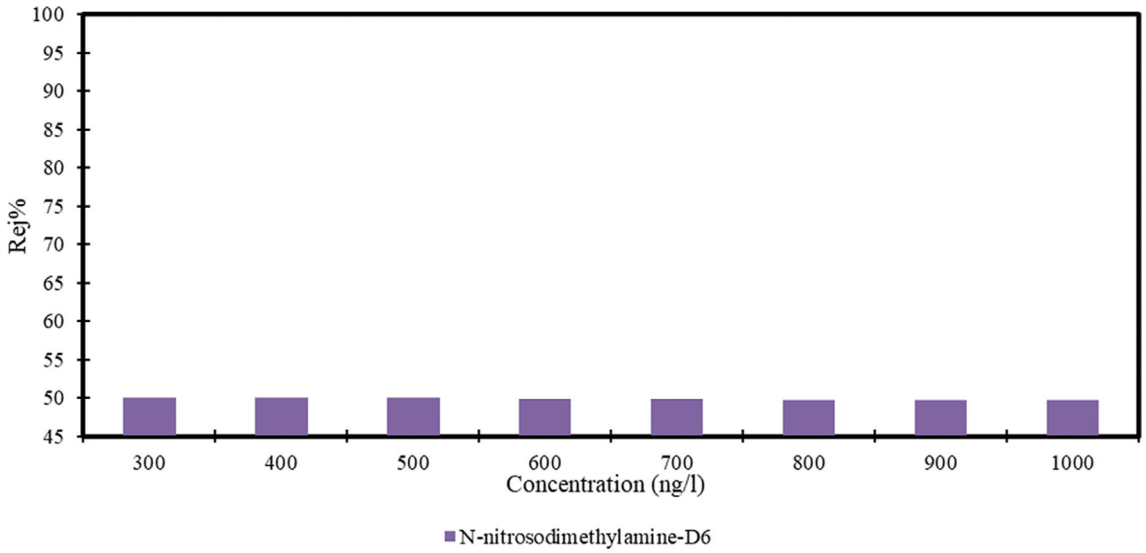

Fig. 6. Variation of N-nitrosodimethylamine-D6 rejection against inlet feed concentration of N-nitrosodimethylamine-D6 at fixed feed flowrate, pressure, and temperature (inlet pressure (20 atm), feed flowrate (777.6 m^3/day), and temperature (25 °C)).

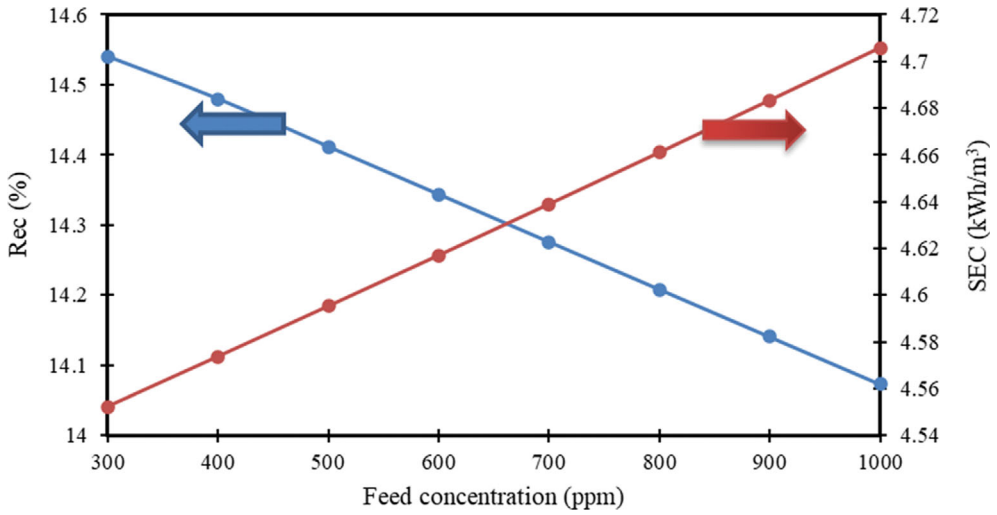

Fig. 7. Variations of water recovery and specific energy consumption against inlet feed concentration of pollutants at fixed feed flowrate, pressure, and temperature (inlet pressure (20 atm), feed flowrate (777.6 m^3/day), and temperature (25 °C)).

centration shown in Table 4. In this regard, Fujioka et al. [31] observed no influence of feed concentration of N-nitrosodimethylamine-D6 on its removal from wastewater. However, it can be stated that both aluminum, chlorophenol, sulphate, dimethylphenol, and NaCl have high rejection values between 89% and 99%. Also, cyanide and aniline have rejection values between 56% and 70%. Finally, N-nitrosodimethylamine-D6 has the lowest rejection below 50%. The low rejections of cyanide, aniline and N-nitrosodimethylamine-D6 are attributed to the high solute transport parameters of these species (Table 2), which identifies the high permeation of these solutes throughout the membrane pores. This increases the solute concentration in the permeate channel and therefore reduces the overall species rejection. Furthermore, Fig. 7 elucidates the actual influence of feed concentration of each pollutant (except N-nitrosodimethylamine-D6) on the water recovery and specific energy consumption of the RO system (Fig. 1). Statistically, Fig. 7 assures insignificant reduction of water recovery of 3.2% and around 3.4% increase of specific energy consumption due to increasing feed concentration from 300 ppm to 1,000 ppm of the considered pollutants. At a fixed inlet feed flow rate, increasing feed concentration results in a rise in osmotic pressure, which slows the overall driving force of water permeation through the membrane pores and reduces water recovery. Similarly, this would progress the specific energy consumption as a consequence of increasing the pollutant concentration. Wang et al. [32] demonstrated the growth of specific energy consumption and decreased water flux of three stages and four stages low-salt-rejection RO process due to increasing feed concentration.

To examine the influence of feed temperature on the rejection of pollutants, water recovery and specific energy consumption, the

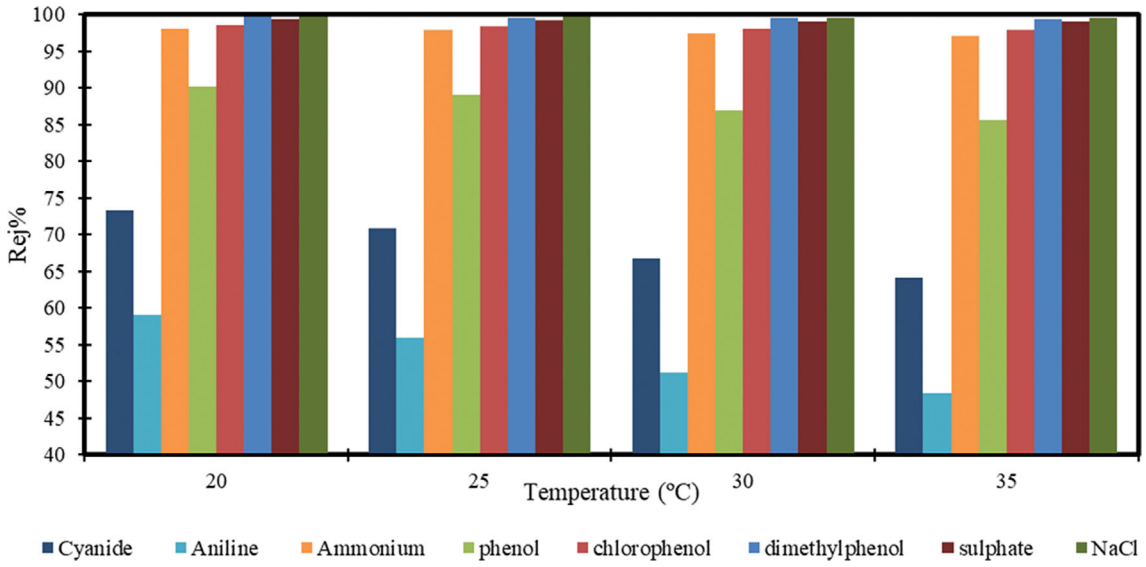

Fig. 8. Variation of solute rejection of different species against feed temperature at fixed feed flowrate, pressure, and concentration of each pollutant (inlet pressure (20 atm), concentration of each pollutant (500 ppm), concentration of N-nitrosodimethylamine-D6 (500 ng/l), and feed flowrate (777.6 m^3/day)).

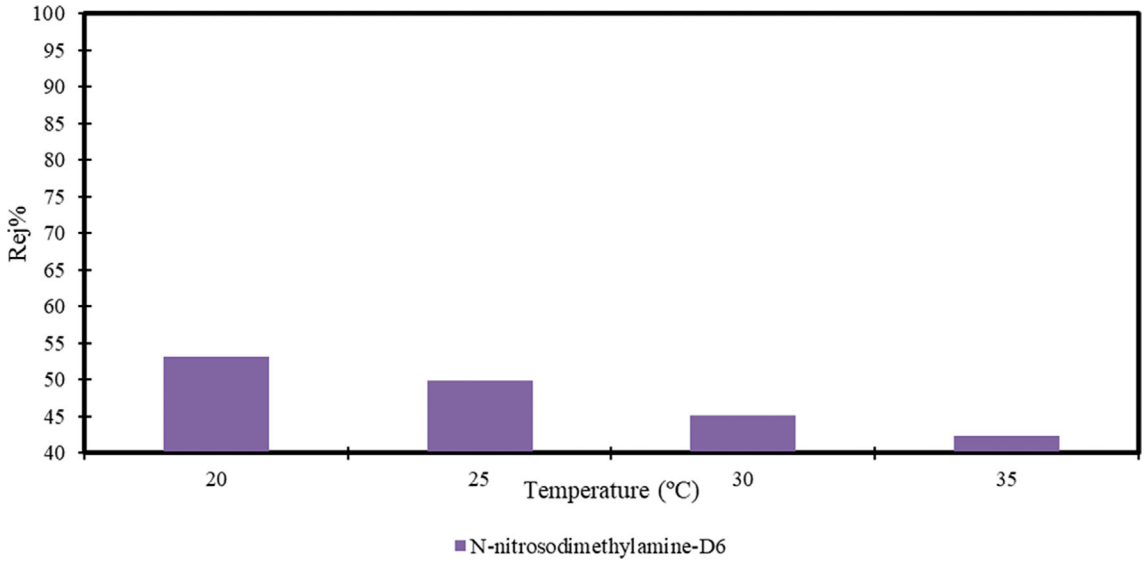

Fig. 9. Variation of N-nitrosodimethylamine-D6 rejection against feed temperature at fixed feed flowrate, pressure, and concentration of N-nitrosodimethylamine-D6 (inlet pressure (20 atm), concentration of N-nitrosodimethylamine-D6 (500 ng/l), and feed flowrate (777.6 m^3/day)).

following simulation was run at a fixed feed flow rate, pressures, and concentration of each pollutant and N-nitrosodimethylamine-D6 as 777.6 m^3/day, 20 atm, and 500 ppm, 500 ng/l, respectively. The RO system was subjected to a set of variable feed temperatures between 20 °C to 35 °C.

Clearly, an increase in feed temperature would cause a reduction of pollutants' rejections (Figs. 8 and 9). Increasing temperature would increase the solute transport parameter of the pollutant (see Eqs. (7), and (8) in Table A1 of Appendix A). This means the growth of solute flux through the membrane pores, which increases pollutant concentration in the permeate channel and retards pollutant rejection. Seemingly, the water transport parameter of the membrane increases due to an increase in the feed temperature besides increasing the molecular mobility of membrane chains, which have altered the membrane geometry (morphology) and provide a regulatory pathway to freely move the particles in the interior of the membrane. This, in turn, would increase the diffusion of individual molecules due to an increase in the radius of a membrane tube and cause an increase of permeated water through the membrane pores, which raises the water recovery at fixed inlet feed flow rate (Fig. 10). The inherent mechanism of the temperature impact on the aromatic polyamide thin film composite RO membrane was

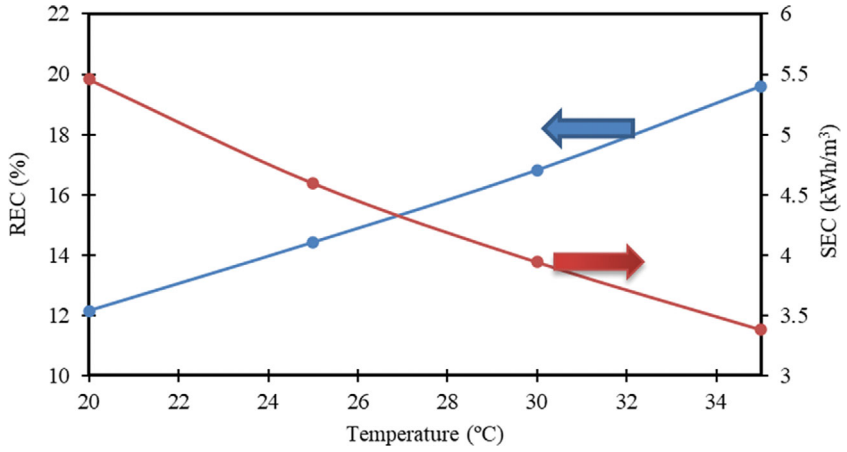

Fig. 10. Variation of water recovery and specific energy consumption against feed temperature at fixed feed flowrate, pressure, and concentration of each pollutant (inlet pressure (20 atm), concentration of each pollutant (500 ppm), concentration of N-nitrosodimethylamine-D6 (500 ng/l), and feed flowrate (777.6 m^3/day)).

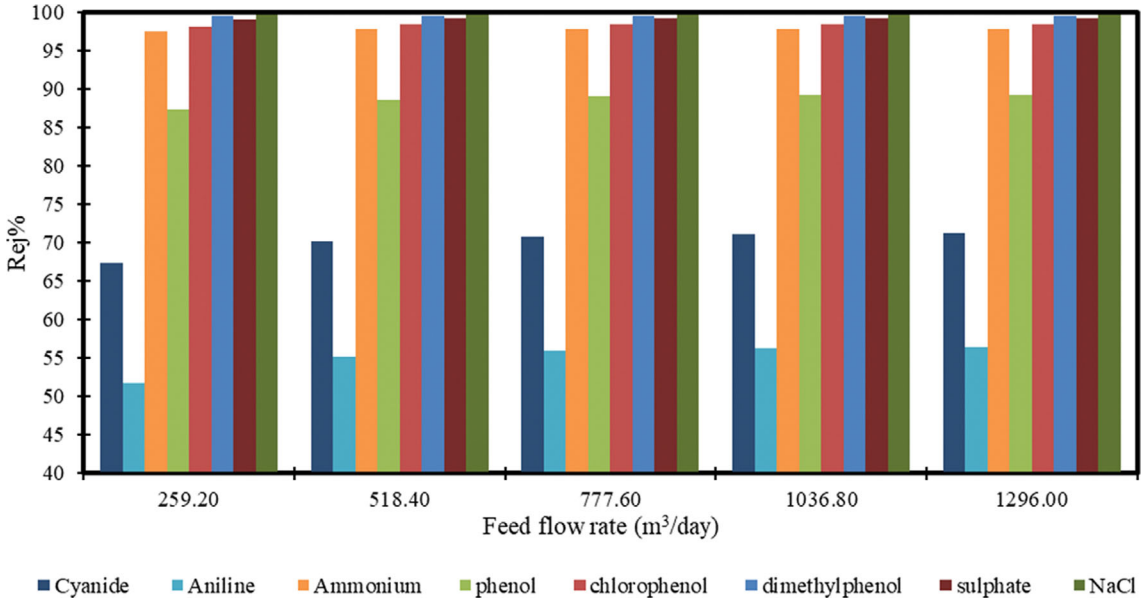

Fig. 11. Variation of solute rejection of different species against feed flow rate at fixed feed pressure, temperature and concentration of each pollutant (inlet pressure (20 atm), concentration of each pollutant (500 ppm), and temperature (25 °C)).

studied by Li et al. [33]. This research provided a comprehensive microscopic understanding of the temperature influence on the dynamics of water and salt ion transport as well as membrane architecture. They stated that pore size distribution becomes more uniform and increases due to increasing the flexibility of membrane chain, which promotes the internal free space as the temperature increases. Thus, it is fair to expect a reduction of specific energy consumption consequently due to increasing the water flux as a result to increasing temperature. Indeed, the increase of feed temperature from 20 °C to 35 °C has a clear influence on the rejections of N-nitrosodimethylamine-D6, aniline, cyanide, and phenol compared to other pollutants. This is due to having high solute transport parameters that introduce a clear influence on the tested rejection parameter. Koutsou et al. [34] stated that increasing water temperature from 15 °C to 40 °C resulted in a reduction of specific energy consumption of a typical single stage RO seawater and brackish water desalination process. This is due to the reductions of viscosity and flow friction losses that improved the water permeation and facilitated the water filtration process.

The influence of inlet feed flow rate of RO system shown in Fig. 1 on the removal of multicomponent is represented in Figs. 11 and 12. The inlet feed flow rate varies between 259.2 m^3/day to 1,296 m^3/day at a fixed set of other operating conditions of 20 atm, 25 °C of pressure and temperature, respectively, 500 ppm of each pollutant and 500 ng/l of N-nitrosodimethylamine-D6. Also, the influences of inlet feed flow rate on the water recovery and specific energy consumption are demonstrated in Fig. 13. Notably, insignificant increase of pollutant removal against the increase of

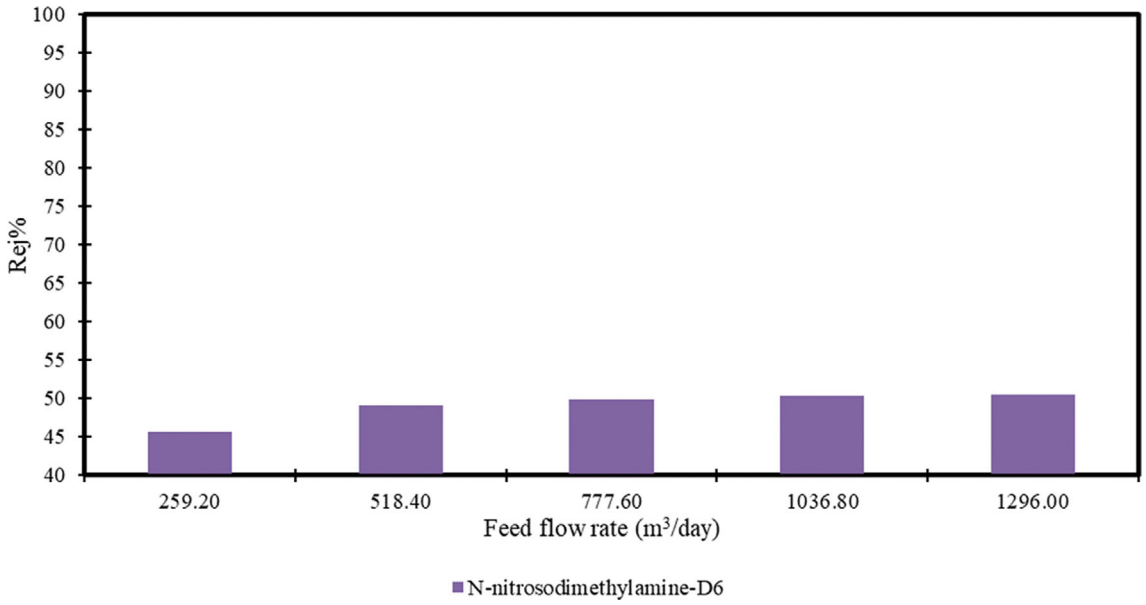

Fig. 12. Variation of N-nitrosodimethylamine-D6 rejection of different species against feed flow rate at fixed feed pressure, temperature and concentration of N-nitrosodimethylamine-D6 (inlet pressure (20 atm), concentration (500 ng/l), and temperature (25 °C)).

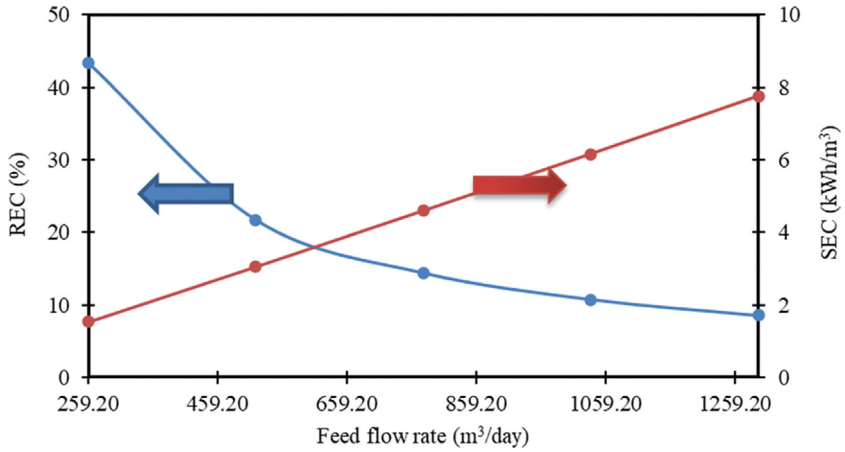

Fig. 13. Variations of water recovery and specific energy consumption against feed flow rate at fixed feed pressure, temperature and concentration of each pollutant (inlet pressure (20 atm), concentration of each pollutant (500 ppm), concentration of N-nitrosodimethylamine-D6 (500 ng/l), and temperature (25 °C)).

inlet feed flow rate can be found in Figs. 11 and 12. This can be attributed to decrease in the rate of accumulation of pollutants on the membrane surface due to increasing the rate of turbulence, i.e., increasing the inlet feed flow rate. This causes a reduction of passing the pollutants throughout the membrane pores and then insignificantly increases the rejection rate accordingly due to decreasing the permeate concentration. However, Fig. 13 demonstrates that water recovery decreases with increasing feed flow rate. Despite having a positive influence of reducing the concentration polarization and osmotic pressure as the feed flow rate rises, the increase of product flow rate is not comparable (much lower) with the increase of feed flow rate. Thus, the water recovery declines with increasing inlet feed flow rate. Accordingly, water recovery shows a noticeable reduction of more than 80%, which is accompanied with a steady increase of specific energy consumption due to insignificant improvement of product flow rate against the progress of feed flow rate (Fig. 13). Abbas [35] concluded the same results through the simulation and analysis of an industrial water desalination plant of brackish water spiral-wound membrane modules.

The simulation results of Figs. 2 to 13 can be compared, and the results show that increasing feed pressure has a greater impact on the rejection of pollutants than increasing feed concentration, temperature, or flow rate. In contrast to feed concentration and temperature, which allowed for a reduction in the removal of pollutants, note that the rejections of pollutants increase as feed pressure and inlet flow rate increase. Furthermore, the water recovery has improved as a result of rising feed pressure and temperature as opposed to declining as feed concentration and feed flow rate increased. For

the specific energy usage, the findings are the exact opposite.

It is acceptable to acknowledge that the simulation findings must be taken into consideration for further improvement in order to understand the most crucial operational components of RO system under varying operating situations. To explore the boundaries of ideal operating parameters suitable for the highest rejections of contaminants existing at various feed concentrations, the RO process will be optimized in the next section.

OPTIMIZATION OF THE OPERATING CONDITIONS OF RO PROCESS TOWARDS THE HIGHEST SIMULTANEOUS REMOVAL OF POLLUTANTS FROM WASTEWATER

The improvement of the reverse osmosis system, as depicted in Fig. 1, is a crucial effort that should be focused on ensuring the simultaneous removal of the most pollutants possible. As a result, the focus of this section is on identifying the ideal operating conditions that would fulfill the ultimate values of rejections for pollutants ($Rej_{(pollutants)}$) while taking into account the lower and upper bounds of the decision variables. The optimization was specifically carried out for a range of inlet feed concentrations of pollutants (C_f) between 500 ppm and 1,000 ppm, and between 500 ng/l and 100 ng/l of N-nitrosodimethylamine-D6 at a constant feed temperature (T) of 25 °C. In light of this, the decision variables of feed pressure (P_f) and flow rate (Q_f) are the ones that would be reasonable to achieve the best pollutant rejection. The simulation results of Figs. 4, 7, 10 and 13 indicate that the lowest specific energy consumption is 1.528 kwh/m^3 while the average specific energy consumption (SEC) of the whole readings is 4.55 kwh/m^3. Thus, it has been decided to consider the medium value of 3 kwh/m^3 as the targeted specific energy consumption, which is considered as an equality constraint.

Based on this, the mathematical formula of the optimization would be as follows:

The objective function:

$$\underset{P_f,\, Q_f}{\text{Max}} \quad Rej_{(pollutants)}$$

Subject to

1 - Inequality constraints for the inlet stage:

$$10 \text{ atm} \le P_f \le 81 \text{ atm}$$
$$259.2 \text{ m}^3/\text{day} \le Q_f \le 1{,}390.17 \text{ m}^3/\text{day}$$

2 - Inequality constraints of each element of spiral wound membrane:

$$Q_f^L \le Q_f \le Q_f^U$$

3 - Equality constraint:

$$\text{Process Model} \quad f(x, u, v)=0$$
$$\text{SEC}=3 \text{ kwh/m}^3$$

Table 5 demonstrates the optimization results including the optimal operating conditions of feed flow rate and pressure that suit the maximum removal values of associated pollutants for three cases of feed concentrations at fixed feed temperature of 25 °C. In this regard, it can be stated that the optimization has enabled to increase the removal of the pollutants in different ratios compared to the simulation results. Also, the optimum removal values are obtained with considering the constraints of decision variables and equality constraint of specific energy consumption of 3 kWh/m^3. Table 5 ascertains the importance of adjusting the optimal values of the decision variables to accommodate the variation of feed concentration of the considered pollutants. To ensure the production of the right product flow rate with increased feed concentrations, which involves a fixed specific energy consumption as specified, the feed flow rate must specifically be reduced within negligible reduction in feed pressure.

Despite the improvement of removing several pollutants, there

Table 5. Optimization results of selected pollutants compounds at three different feed concentrations at fixed temperature of 25 °C

Feed concentration									
500 ppm				700 ppm				1,000 ppm			
Species	Optimum decision variables		Max.	Species	Optimum decision variables		Max.	Species	Optimum decision variables		Max.
	P_f	Q_f	Rej		P_f	Q_f	Rej		P_f	Q_f	Rej
Cyanide			83.27	Cyanide			83.22	Cyanide			83.13
Aniline			72.05	Aniline			71.96	Aniline			71.84
Ammonium			98.94	Ammonium			98.94	Ammonium			98.93
Phenol			94.37	Phenol			94.35	Phenol			94.31
Chlorophenol			99.23	Chlorophenol			99.23	Chlorophenol			99.22
Dimethylphenol	64.1	537.8	99.79	Dimethylphenol	64.0	535.77	99.79	Dimethylphenol	63.9	532.72	99.79
Sulphate			99.64	Sulphate			99.63	Sulphate			99.63
NaCl			99.84	NaCl			99.84	NaCl			99.84
N-nitrosodimethylamine-D6 (500 ng/l)			66.78	N-nitrosodimethylamine-D6 (ng/l)			66.69	N-nitrosodimethylamine-D6 (ng/l)			66.56

is still room for improvement in the elimination of some pollutants, such as aniline and N-nitrosodimethylamine-D6. This shows that the RO system's setup must be modified in order to improve the rejection of these pollutants. The permeate reprocessing design of RO system can be accomplished to enhance the removal of subborned pollutants such as aniline and N-nitrosodimethylamine-D6. This is specifically characterized by processing the permeate stream of the first stage to the next stage with utilizing a booster pump to increase the feed pressure on the second stage. Al-Obaidi et al. [36] conducted a thorough simulation and optimization study to analyze the performance of a conceptual design of multi pass multi stage permeate reprocessing design to remove N-nitrosodimethylamine-D6 from wastewater and to maximize the removal, respectively. This, in turn, has introduced the maximum rejection of 92.49% of N-nitrosodimethylamine-D6.

CONCLUSIONS

In particular, the wastewater effluents of several industries contain a diversity of nonorganic and organic compounds that need to be removed before disposing into surface water. The RO process and, especially, spiral wound module has elaborated its efficiency in removing pollutants from wastewater. A comprehensive model-based simulation was established for a multistage spiral wound module of RO process to specifically treat multicomponent wastewater. The effects of inlet conditions of RO process on the elimination of associated pollutants were evaluated with estimating the overall water recovery and specific energy consumption. To systematically improve the rejection of the selected compounds, the model was embedded in an optimization methodology. Accordingly, the optimal conditions were investigated to provide the highest rejection with accommodating a plausible value of specify energy consumption.

NOMENCLATURE

A_m : effective membrane area [m^2]
$A_{w(T)}$: water transport parameter [m/atm s]
A' : spacer characteristics [Non]
$B_{s(T)}$: solute transport parameter [m/s]
C_b : bulk solute concentration [ppm]
C_f : feed solute concentration [ppm]
C_w : solute concentration on the membrane surface [ppm]
C_p : solute concentration in the permeate side [ppm]
C_r : solute concentration in the discharged line [ppm]
C_{td} : total drag coefficient [dimensionless]
D_b : solute diffusion parameter of feed at the feed side [m^2/s]
d_h : hydraulic diameter [m]
Q_s : solute flux [kg/m^2 s]
J_w : water flux [m/s]
k : mass transfer coefficient [m/s]
k_{dc} : constant in Eq. (14) of Table A1 of Appendix A [Non]
L : length of the membrane [m]
m_f : parameter in Eq. (16) of Table A1 of Appendix A [Non]
n : spacer characteristics [Non]
P_f : feed pressure [atm]
P_r : retentate pressure [atm]
P_p : permeate pressure [atm]
Q_b : bulk feed flow rate [m^3/day]
Q_f : feed flow rate [m^3/day]
Q_p : permeate flow rate [m^3/day]
Q_r : retentate flow rate [m^3/day]
Re_b : reynolds number [Non]
Rec : water recovery [Non]
Rej : solute rejection [Non]
T : feed temperature [°C]
t_f : height of feed channel [m]
U_b : bulk feed velocity [m/s]
W : width of the membrane [m]

Subscript

μ_b : bulk viscosity [kg/m s]
ρ_b : bulk density [kg/m^3]
$\Delta P_{drop,E}$: pressure drop of the membrane module [atm]
π_b : bulk osmotic pressure [atm]
π_p : permeate osmotic pressure [atm]
ε : void fraction of the spacer [Non]

FUNDING

This study was not funded.

CONFLICT OF INTEREST

The author declares that he has no conflict of interest.

REFERENCES

1. R. Mukherjee and S. De, *Sep. Purif. Technol.*, **157**, 229 (2016).
2. M. Al-Obaidi, C. Kara-Zaitri and I. M. Mujtaba, *Wastewater treatment by reverse osmosis process*, CRC Press (2020).
3. T. Fujioka, K. P. Ishida, T. Shintani and H. Kodamatani, *Water Res.*, **131**, 45 (2018).
4. K. Madwar and H. Tarazi, *Desalination*, **152**(1-3), 325 (2003).
5. A. J. Toth, *Membranes*, **10**(10), 265 (2020).
6. R. W. Baker, *Membrane technology and applications*, 2nd ed. Membrane Technology and Research, Inc. California (2004).
7. N. Al-Bastaki, *Chem. Eng. Process.*, **43**, 1561 (2004).
8. A. L. Ahmad, M. F. Chong and S. Bhatia, *Chem. Eng. J.*, **132**(1-3), 183 (2007).
9. J. H. Al-Rifai, H. Khabbaz and A. I. Schäfer, *Sep. Purif. Technol.*, **77**(1), 60 (2011).
10. T. Fujioka, S. J. Khan, J. A. McDonald, A. Roux, Y. Poussade, J. E. Drewes and L. D. Nghiem, *Water Res.*, **47**(16), 6141 (2013).
11. L. Wang, Y. Sun and B. Chen, *Water Res.*, **144**, 383 (2018).
12. M. A. Al-Obaidi, C. Kara-Zaïtri and I. M. Mujtaba, *Comput. Aided Chem. Eng.*, **44**, 1867 (2018).
13. J. M. Domingos, G. A. Martinez, E. Morselli, S. Bandini and L. Bertin, *Sep. Purif. Technol.*, **290**, 120840 (2022).
14. G. Filippini, M. A. Al-Obaidi, F. Manenti and I. M. Mujtaba, *Desalination*, **448**, 21 (2018).
15. M. A. Al-Obaidi, G. Filippini, F. Manenti and I. M. Mujtaba, *Desali-*

nation, **456**, 136 (2019).
16. R. Maleki, N. Koukabi and E. Kolvari, *Appl. Organomet. Chem.*, **32**(1), e3905 (2018).
17. A. A. Gami, M. Y. Shukor, K. A. Khalil, F. A. Dahalan, A. Khalid and S. A. Ahmad, *J. Environ. Microbiol. Toxicol.*, **2**(1), 11 (2014).
18. A. Bódalo, J. L. Gómez, E. Gómez, G. León and M. Tejera, *Desalination*, **168**, 277 (2004).
19. A. M. Hidalgo, G. León, M. Gómez, M. D. Murcia, M. D. Bernal and S. Ortega, *Environ. Technol.*, **35**(9), 1175 (2014).
20. A. Bódalo, J. L. Gómez, E. Gómez, G. León and M. Tejera, *Desalination*, **184**, 149 (2005).
21. G. Srinivasan, S. Sundaramoorthy and D. V. R. Murthy, *Am. J. Eng. Appl. Sci.*, **3**(1), 31 (2010).
22. S. Sundaramoorthy, G. Srinivasan and D. V. R. Murthy, *Desalination*, **277**(1-3), 257 (2011).
23. M. A. Al-Obaidi, C. Kara-Zaïtri and I. M. Mujtaba, *J. Clean. Prod.*, **193**, 140 (2018).
24. M. A. Al-Obaidi, C. Kara-Zaitri and I. M. Mujtaba, *J. Environ. Chem. Eng.*, **6**(4), 4797 (2018).
25. A. Bódalo, J. L. Gómez, E. Gómez, G. León and M. Tejera, *Desalination*, **162**, 55 (2003).
26. M. Wilf and K. Klinko, *Desalination*, **138**(1-3), 299 (2001).
27. D. L. Sedlak, R. A. Deeb, E. L. Hawley, W. A. Mitch, T. D. Durbin, S. Mowbray and S. Carr, *Water Environ. Res.*, **77**(1), 32 (2005).
28. G. Srinivasan, S. Sundaramoorthy and D. R. Murthy, *Desalination*, **281**, 199 (2011).
29. Y. Cui, X. Y. Liu, T. S. Chung, M. Weber, C. Staudt and C. Maletzko, *Water Res.*, **91**, 104 (2016).
30. A. J. Karabelas, C. P. Koutsou, M. Kostoglou and D. C. Sioutopoulos, *Desalination*, **431**, 15 (2018).
31. T. Fujioka, L. D. Nghiem, S. J. Khan, J. A. McDonald, Y. Poussade and J. E. Drewes, *J. Membr. Sci.*, **409**, 66 (2012).
32. Z. Wang, A. Deshmukh, Y. Du and M. Elimelech, *Water Res.*, **170**, 115317 (2020).
33. K. Li, L. Liu, H. Wu, S. Li, C. Yu, Y. Zhou, W. Huang and D. Yan, *Phys. Chem. Chem. Phys.*, **20**(47), 29996 (2018).
34. C. P. Koutsou, E. Kritikos, A. J. Karabelas and M. Kostoglou, *Desalination*, **476**, 114213 (2020).
35. A. Abbas, *Chem. Eng. Process.: Process Intensification*, **44**(9), 999 (2005).
36. M A. Al-Obaidi, C. Kara-Zaitri and I. M. Mujtaba, *J. Environ. Chem. Eng.*, **6**(4), 4797 (2018).

APPENDIX A

Table A1. Modelling of an individual spiral wound RO membrane [14,15]

Model equations	Specifications	Eq. no
$Q_p = A_{w(T)}\left(P_f - \frac{\Delta P_{drop,E}}{2} - P_p - \pi_w - \pi_p\right)A_m$	Total permeate flow rate	1
$Q_s = B_{s(T)}(C_w - C_p)$	Total solute flux	2
$\pi_w = 0.76881\ C_w \quad \pi_p = 0.7994\ C_p$	Osmotic pressure of the feed and permeate channels	3, 4
$A_{w(T)} = A_{w(25\,C)}\ \exp[0.0343\ (T-25)]$ <25 °C	Impact of temperature on water transport parameters	5
$A_{w(T)} = A_{w(25\,C)}\ \exp[0.0307\ (T-25)]$ >25 °C	Impact of temperature on water transport parameters	6
$B_{s(T)} = B_{s(25\,C)}(1+0.08\ (T-25))$ <25 °C	Impact of temperature on solute transport parameters	7
$B_{s(T)} = B_{s(25\,C)}(1+0.05\ (T-25))$ >25 °C	Impact of temperature on solute transport parameters	8
$\Delta P_{drop,E} = \frac{9.869\times10^{-6} A' \rho_b Q_b^2 L}{2 d_h Re_b^{n^*} (W t_f \varepsilon)^2}$	Pressure drop per element	9
$Re_b = \frac{\rho_b d_h Q_b}{t_f W \mu_b}$	Reynolds number	10
$Q_b = \frac{Q_f + Q_r}{2}$	Bulk flow rate	11
$C_b = \frac{C_f + C_r}{2}$	Bulk concentration	12
$\frac{(C_w - C_p)}{(C_b - C_p)} = \exp\left(\frac{Q_p/A_m}{k}\right)$	Wall membrane concentration	13
$k = 0.664 k_{dc} Re_b^{0.5} Sc^{0.33}\left(\frac{D_b}{d_h}\right)\left(\frac{2d_h}{L_f}\right)^{0.5}$	Mass transfer coefficient	14
$Sc = \frac{\mu_b}{\rho_b D_b}$	Schmidt number	15
$\rho_b = 498.4 m_f + \sqrt{[248{,}400 m_f^2 + 752.4 m_f C_b]}$	Feed density	16
$m_f = 1.0069 - 2.757\times10^{-4} T$	Parameter in Eq. (16)	17
$D_b = 6.725\times10^{-6} \exp\left\{0.1546\times10^{-3} C_b - \frac{2{,}513}{T+273.15}\right\}$	Diffusivity parameter	18
$\mu_b = 1.234\times10^{-6} \exp\left\{0.0212 C_b + \frac{1{,}965}{T+273.15}\right\}$	Viscosity parameter	19
$Q_f = Q_r + Q_p$	Total mass balance	20
$Q_f C_f - Q_r C_r = Q_p C_p$	Total solute balance	21
$C_p = \frac{B_s C_f e^{J_w/k}}{J_w + B_s e^{J_w/k}}$	Permeate concentration	22
$Rec = \frac{Q_p}{Q_f}$	Recovery rate	23
$Rej = \frac{C_f - C_p}{C_f}$	Solute rejection	24

Table A2. Modelling of multi-stage direct pass operation of RO seawater desalination plant

Model equations	Specifications	Eq. no
$Q_{f(plant)}=Q_{r(plant)}+Q_{p(plant)}$	Plant feed flow rate	1
$Q_{f(plant)}C_{f(plant)}=Q_{r(plant)}C_{r(plant)}+Q_{p(plant)}C_{p(plant)}$	Plant feed concentration	2
$Q_{r(plant)}=Q_{r(Stage\ 3)}$	Plant retentate flow rate	3
$C_{r(plant)}=C_{r(Stage\ 3)}$	Plant retentate concentration	4
$C_{p(plant)}=\frac{C_{p(Stage\ 1)}Q_{p(Stage\ 1)}+C_{p(Stage\ 2)}Q_{p(Stage\ 2)}+C_{p(Block\ 3)}Q_{p(Stage\ 3)}}{Q_{p(plant)}}$	Plant product concentration	5
$Q_{p(plant)}=Q_{p(Stage\ 1)}+Q_{p(Stage\ 2)}+Q_{p(Stage\ 3)}$	Plant permeate flow rate	6
$T_{f(plant)}=T_{r(plant)}$	Plant constant temperature	7
$P_{f(plant)}=P_{f(Stage\ 1)}$	Plant feed pressure	8
$P_{r(plant)}=P_{r(Stage\ 3)}$	Plant retentate pressure	9
$Rec_{(plant)}=\frac{Q_{p(plant)}}{Q_{f(plant)}}\times 100$	Total plant permeate recovery	10
$Rej_{(plant)}=\frac{C_{f(plant)}-C_{p(plant)}}{C_{f(plant)}}\times 100$	Total plant rejection	11
$C_{f(Stage\ 1)}=C_{f(plant)}$	Feed concentration of 1st Stage	12
$Q_{f(Stage\ 1)}=Q_{f(plant)}$	Feed flow rate of 1st Stage	13
$Q_{p(Stage\ 1)}=\sum_{PV=1}^{20}Q_{p(PV)}$	Permeate flow rate of 1st Stage	14
$C_{p(Stage\ 1)}=\frac{\sum_{PV=1}^{20}C_{p(PV)}Q_{p(PV)}}{Q_{p(Stage\ 1)}}$	Permeate concentration of 1st Stage	15
$Rej_{(Stage\ 1)}=\frac{C_{f(Stage\ 1)}-C_{p(Stage\ 1)}}{C_{f(Stage\ 1)}}\times 100$	Total solute rejection of 1st Stage	16
$Rec_{(Stage\ 1)}=\frac{Q_{p(Stage\ 1)}}{Q_{f(Stage\ 1)}}\times 100$	Total permeate recovery of 1st Stage	17
$SEC=\frac{\frac{((P_{f(plant)}\times 101{,}325)Q_{f(plant)})}{Q_{p(plant)}\varepsilon_{pump}}}{36\times 10^5}$	Total plant specific energy consumption	18